

# One-dimensional fermions with incommensuration

Diptiman Sen <sup>\*</sup> and Siddhartha Lal <sup>†</sup>

*Centre for Theoretical Studies, Indian Institute of Science,  
Bangalore 560012, India*

We study the spectrum of fermions hopping on a chain with a weak incommensuration close to dimerization; both  $q$ , the deviation of the wave number from  $\pi$ , and  $\delta$ , the strength of the incommensuration, are small. For free fermions, we use a continuum Dirac theory to show that there are an infinite number of bands which meet at zero energy as  $q$  approaches zero. In the limit that the ratio  $q/\delta \rightarrow 0$ , the number of states lying inside the  $q = 0$  gap is nonzero and equal to  $2\delta/\pi^2$ . Thus the limit  $q \rightarrow 0$  differs from  $q = 0$ ; this can be seen clearly in the behavior of the specific heat at low temperature. For interacting fermions or the  $XXZ$  spin-1/2 chain close to dimerization, we use bosonization to argue that similar results hold; as  $q \rightarrow 0$ , we find a nontrivial density of states near zero energy. However, the limit  $q \rightarrow 0$  and  $q = 0$  give the same results near commensurate wave numbers which are *different* from  $\pi$ . We apply our results to the Azbel-Hofstadter problem of electrons hopping on a two-dimensional lattice in the presence of a magnetic field. Finally, we discuss the complete energy spectrum of noninteracting fermions with incommensurate hopping by going up to higher orders in  $\delta$ .

PACS number: 71.10.Fd, 71.10.Pm, 75.10.Jm

---

<sup>\*</sup>E-mail address: diptiman@cts.iisc.ernet.in

<sup>†</sup>E-mail address: sanjayl@cts.iisc.ernet.in

## I. INTRODUCTION

One-dimensional lattice models with incommensurate hopping elements or on-site potentials have been studied for many years from different points of view<sup>1,2</sup>. Many unusual properties of the quantum spectra and wave functions have been discovered for various kinds of aperiodicity<sup>3</sup>. Physically, such models have applications to several problems such as incommensurate crystals<sup>4</sup>, semiconductor heterojunctions<sup>5</sup>, the incommensurate phase of spin-Peierls systems such as  $CuGeO_3$ <sup>6</sup>, and the Azbel-Hofstadter problem of particles hopping on a two-dimensional lattice in the presence of a magnetic field<sup>7</sup>. If the incommensuration is close to dimerization (wave number  $\pi$ ), then the models have an additional interest in the context of metal-insulator transitions near half-filling and spin-Peierls systems near zero magnetization<sup>8,9</sup>.

In this paper, we study a model of fermions with a hopping which has a *weak* sinusoidal incommensurate term *close* to dimerization. We will show both numerically and analytically that this has some unusual properties, particularly inside the gap which exists *exactly* at dimerization. The major surprise is that states appear inside the gap *as soon as* we move away from dimerization. These states carry a finite weight, and therefore contribute to quantities like the specific heat at low temperatures, as we will show. In Secs. II A and II B, we discuss free fermions or the  $XY$  spin-1/2 chain close to dimerization (and half-filling) for which quantitatively accurate results can be obtained by analytical methods. We will use a continuum Dirac field formulation, followed by perturbation theory and a WKB analysis, to find the locations and widths of the energy bands inside the  $q = 0$  gap; here  $q$  is the deviation from  $\pi$  of the wave number of the incommensuration. In Sec. II C, we will explain how the limit  $q \rightarrow 0$  get reconciled with the results for  $q = 0$  in a somewhat different model, namely, the Azbel-Hofstadter problem in which electrons hop on a two-dimensional lattice in the presence of a magnetic field. In Sec. III, we use bosonization to argue that similar differences between  $q \rightarrow 0$  and  $q = 0$  occur for interacting fermions or the  $XXZ$  spin-1/2 chain, which is the more general and interesting case. In Sec. IV, we show that such peculiarities do not occur in the vicinity of any wave number which is *different* from  $\pi$ . In Sec. V, we consider continuum theories which go up to higher orders in the strength of the incommensuration; this enables us to discuss the complete energy spectrum of fermions with a weak incommensurate hopping. In Sec. VI, we make some concluding remarks.

Our work differs from earlier ones which have concentrated on the effects of incommensuration which are either large or close to “highly” irrational numbers such as the golden ratio<sup>1,3,4,7</sup>. Further, we will use techniques from continuum theory which have not been used much in this area (except for the recent work in Ref. 8).

## II. NONINTERACTING FERMIONS CLOSE TO DIMERIZATION

### A. Numerical results

We begin with the following Hamiltonian for noninteracting and spinless fermions on a lattice

$$\begin{aligned} H &= -\frac{1}{2} \sum_n J_n (c_n^\dagger c_{n+1} + c_{n+1}^\dagger c_n) - \mu \sum_n c_n^\dagger c_n, \\ J_n &= 1 + \delta \cos(\pi + q)n, \end{aligned} \tag{1}$$

where we will assume that  $\delta \ll 1$  and  $q \ll \pi$ . (In that limit, we will show later that it does not matter if the incommensurate term is put in the chemical potential  $\mu$  (i.e., on-site) rather than in the hopping  $J_n$ ). We set  $\mu = 0$  as we are interested in energies close to zero. If  $\delta = 0$ , the model can be easily solved; the dispersion relation is  $E(k) = -\cos k$ . In the ground state, all the states with momenta lying in the range

$[-k_F, k_F]$  are filled, where the Fermi momentum  $k_F = \pi/2$ . The Fermi velocity is equal to  $\sin k_F = 1$ . (We will set both the lattice spacing and Planck's constant equal to 1).

If  $\delta \neq 0$  but  $q = 0$ , i.e., with dimerization, the model can still be solved analytically. There is an energy gap extending from  $-\delta$  to  $\delta$ . Let us now consider nonzero values of  $q$ . [Since  $\cos(\pi+q)n = \cos(qn)\cos(\pi n)$ , we see that a small value of  $q$  is equivalent to dimerization term whose amplitude  $\delta \cos(qn)$  varies slowly with  $n$ ]. For any rational value of  $q/\pi = M/N$ , where  $M$  and  $N$  are relatively prime integers, we have a periodic system with period  $P$  equal to  $N$  if  $M + N$  is even and  $2N$  if  $M + N$  is odd. The one-particle spectrum of Eq. (1) can be found by solving the discrete Schrödinger equation

$$-\frac{1}{2} [ J_n \psi_{n+1} + J_{n-1} \psi_{n-1} ] = E \psi_n , \quad (2)$$

which is equivalent to the equation

$$\begin{pmatrix} \psi_{n+1} \\ \psi_n \end{pmatrix} = \begin{pmatrix} -2E/J_n & -J_{n-1}/J_n \\ 1 & 0 \end{pmatrix} \begin{pmatrix} \psi_n \\ \psi_{n-1} \end{pmatrix} . \quad (3)$$

The allowed values of energy can therefore be found by computing the transfer matrix  $M(q, E)$  obtained by multiplying together  $P$  matrices<sup>3</sup>,

$$M(q, E) = \prod_{n=1}^P \begin{pmatrix} -2E/J_n & -J_{n-1}/J_n \\ 1 & 0 \end{pmatrix} . \quad (4)$$

Since  $\det M(q, E) = 1$  and  $\text{tr} M(q, E)$  is real, it is clear that the eigenvalues of  $M(q, E)$  must be either of the form  $r$  and  $1/r$ , or of the form  $\exp(ir)$  and  $\exp(-ir)$ , where  $r$  is real in either case. In the former case, the wave functions  $\psi_n$  diverge exponentially as  $n \rightarrow \infty$  or  $-\infty$ ; hence they are not allowed physically. In the latter case, the wave functions do not diverge at infinity and are allowed. Thus, if  $|\text{tr} M(q, E)| = 2|\cos r| \leq 2$ , the energy  $E$  is allowed in the spectrum; otherwise that energy is not allowed. By following this method and sweeping through a large number of values of  $q$  and  $E$ , we obtain the picture of energy bands and gaps (shaded and unshaded regions, respectively) shown in Figs. 1 and 2, taking  $\delta = 0.05$ . [We have sampled the energy values with a resolution of  $dE = 10^{-6}$ . It may be useful to clarify here that the numerous *vertical* gaps in Figs. 1, 2, 5, 6 and 7 have no physical significance; they are present because we have omitted the regions of  $q/\pi$  whose rational approximations have such long periods  $P$  that a numerical computation would have taken too long]. We have scaled both  $E$  and  $q$  in units of  $\delta$  because the pictures turn out to depend only on those two ratios. We immediately see that the pictures look much more complicated than the situation in which  $q$  is *exactly* equal to zero; in that case, there is precisely one gap extending from  $E/\delta = 0$  to 1. [We will consider only positive values of  $q$  and  $E$  since the spectrum is invariant under either  $q \rightarrow -q$  (as is clear from (1)) or  $E \rightarrow -E$ ; the latter is clear from the invariance of  $|\text{tr} M(q, E)|$  under an unitary transformation by the Pauli matrix

$$\sigma^3 = \begin{pmatrix} 1 & 0 \\ 0 & -1 \end{pmatrix} \quad (5)$$

which reverses the sign and simultaneously converts  $E \rightarrow -E$  for each of the  $P$  matrices appearing in (4). Thus the energy bands shown in Figs. 1 and 2 should be understood as continuing to negative values of both  $E$  and  $q$  by reflection about those two axis].

Fig. 1 shows that as  $q/\delta$  increases, the gaps shrink rapidly. We will show that this can be understood using perturbation theory to  $n^{\text{th}}$  order, where  $n$  is an odd integer, and that the gaps shrink as  $(\delta/q)^n$ . We have therefore labeled the gaps in Fig. 1 by the integers  $n = 1, 3, 5, \dots$ . More interestingly, we observe that all the bands approach the origin  $(q, E) = (0, 0)$ . The widths of the low-lying bands vanish exponentially fast as  $q/\delta \rightarrow 0$  as we will argue from a WKB analysis. This makes it impossible to find these portions of

the bands by looking for energies satisfying  $|\text{tr} M(q, E)| \leq 2$  using any reasonable energy resolution  $dE$ . We therefore find these thin portions of the bands by looking for *minima* of  $\text{tr} M^2(q, E)$  as functions of  $E$ . If the energy resolution was infinitesimal, these minima would be found at  $\text{tr} M^2(q, E) = 2 \cos(2r) = -2$ , i.e.,  $\text{tr} M(q, E) = 2 \cos r = 0$ , which occurs inside an energy band. In practice, due to the finite energy resolution  $dE$ , these minima numerically yield single points in energy which lie within a distance of  $dE$  of a band. We are thus able to find the locations of the thin regions without having to use a resolution smaller than  $dE = 10^{-6}$ . In Fig. 2, we show these points (thin regions) which smoothly join on to the wider regions of the bands. We also show six curves which are the analytical results of a low-energy theory of the model which involves solving a 1 + 1-dimensional Dirac equation in a periodic potential. We will also prove that the number of bands in the region  $0 \leq E/\delta \leq 1$  increases as  $2\delta/\pi q$  as  $q/\delta \rightarrow 0$ , while the number of states in each band is equal to  $q/\pi$  when normalized appropriately in the thermodynamic limit, i.e., the number of sites  $L \rightarrow \infty$ . This will show that the number of states lying inside the  $q = 0$  gap is finite and equal to  $2\delta/\pi^2$  in the limit  $q \rightarrow 0$ ; this implies that  $q = 0$  is a rather singular point.

## B. Analytical results

To begin, let us write the Hamiltonian in (1) as a sum  $H = H_0 + V_\delta$ , where  $V_\delta$  is the incommensurate term

$$V_\delta = -\frac{\delta}{2} \sum_n \cos(Qn) (c_n^\dagger c_{n+1} + c_{n+1}^\dagger), \quad (6)$$

where  $Q = \pi + q$  in this section. If

$$|k\rangle = \frac{1}{\sqrt{L}} \exp(ikn) |n\rangle \quad (7)$$

denotes a momentum eigenstate of  $H_0$ , then the matrix elements of  $V_\delta$  are given by

$$\langle k_1 | V_\delta | k_2 \rangle = -\frac{\delta}{4} (\delta_{Q+k_1, k_2} + \delta_{Q+k_2, k_1}) (e^{-ik_1} + e^{ik_2}). \quad (8)$$

Let us understand the gaps for large values of  $q/\delta$  by using perturbation theory about  $\delta = 0$ . If  $q$  and  $\delta$  are both small, the states close to zero energy are dominated by momenta near  $\pm\pi/2$ . Since the incommensuration term  $V_\delta$  in (6) has Fourier components at momenta  $\pm(\pi + q)$ , we see that the gaps above zero energy result from the breaking of the energy degeneracy between the two states with momenta  $k_1 = \pi/2 + nq/2$  and  $k_{n+1} = -\pi/2 - nq/2$ , where  $n = 1, 3, 5, \dots$ . These two states are connected to each other through the  $n - 1$  successive intermediate states with momenta  $k_2 = -\pi/2 + (n - 2)q/2$ ,  $k_3 = \pi/2 + (n - 4)q/2$ ,  $k_4 = -\pi/2 + (n - 6)q/2$ , ...,  $k_n = \pi/2 - (n - 2)q/2$ , since we must have  $k_{j+1} - k_j = \pm(\pi + q) \bmod 2\pi$ . Since all the matrix elements  $\langle k_{j+1} | V_\delta | k_j \rangle$  are approximately equal to  $\pm i\delta/2$  (for  $j = 1, 2, \dots, n$ ) for small values of  $q$  in Eq. (8), and all the energy denominators  $E_j - E_1$  are of the order of  $q$  (for  $j = 2, 3, \dots, n$ ), we see that the two-fold degeneracy (at the energy  $E_1 = E_{n+1} \simeq nq/2$ ) gets broken at the  $n^{\text{th}}$  order in perturbation theory to produce a gap of the order of  $\delta^n/q^{n-1}$ . To be explicit, we find that the upper and lower edges of the two gaps labeled by  $n = 1$  and 3 in Fig. 1 are given by

$$\begin{aligned} \frac{E_\pm(1)}{\delta} &= \frac{q}{2\delta} \pm \frac{1}{2}, \\ \frac{E_\pm(3)}{\delta} &= \frac{3q}{2\delta} + \frac{3\delta}{16q} \pm \frac{\delta^2}{32q^2}, \end{aligned} \quad (9)$$

and we have verified that this agrees well with the numerically obtained boundaries. We can show that the general formula for the gap  $\Delta E(n) = E_+(n) - E_-(n)$  labeled by the odd integer  $n = 2p + 1$  is given by

$$\frac{\Delta E(n)}{\delta} = \frac{2}{\delta} \left| \frac{\prod_{j=1}^n \langle k_{j+1} | V_\delta | k_j \rangle}{\prod_{j=2}^n (E_1 - E_j)} \right| = \frac{(\delta/4q)^{2p}}{(p!)^2} \quad (10)$$

to lowest order in  $\delta$ .

We can count the number of states in the band lying between gaps  $n$  and  $n + 2$  as follows. For  $\delta = 0$ , let us normalize the number of states so that the total number is 1; since the momentum  $k$  goes from  $-\pi$  to  $\pi$  in that case, the density of states in momentum space is  $1/(2\pi)$ . If we now turn on a very small value of  $\delta$ , we find that the band lying between the gaps  $n$  and  $n + 2$  is made up of linear combinations of the states lying between the two momenta intervals  $[\pi/2 + nq/2, \pi/2 + (n + 2)q/2]$  and  $[-\pi/2 - nq/2, -\pi/2 - (n + 2)q/2]$ . The total number of states in these two intervals is  $2(q/2\pi) = q/\pi$ . Thus each band contains  $q/\pi$  states. Now, this number cannot change if we change  $\delta$ , and we can therefore use the same number below in the opposite limit where  $q/\delta$  is small.

Let us examine the more interesting regime where  $q/\delta$  is small and  $E/\delta < 1$ . For analyzing this, it is useful to consider the continuum limit. In this limit, the Fermi field  $\psi(x) = c_n$  can be written as

$$\psi(x) = \psi_R(x) \exp\left(\frac{i\pi x}{2}\right) + \psi_L(x) \exp\left(-\frac{i\pi x}{2}\right), \quad (11)$$

where  $\psi_R$  and  $\psi_L$  denote the right- and left-moving fields, respectively; they vary slowly on the scale of the lattice spacing. We substitute (11) in Eq. (1) and drop terms like  $\exp(\pm i\pi x)$  which vary rapidly. We then find the following Dirac-like equations for the two time-dependent (Heisenberg) fields

$$\begin{aligned} i (\partial/\partial t + \partial/\partial x) \psi_R - i\delta \cos(qx) \psi_L &= 0, \\ i (\partial/\partial t - \partial/\partial x) \psi_L + i\delta \cos(qx) \psi_R &= 0. \end{aligned} \quad (12)$$

The energy spectrum can be found from (12) by defining  $\psi_\pm = \psi_R \pm \psi_L$  which satisfy the equations

$$\begin{aligned} [ -\partial^2/\partial x^2 + \delta^2 \cos^2(qx) - \delta q \sin(qx) ] \psi_+ &= E^2 \psi_+, \\ [ -\partial^2/\partial x^2 + \delta^2 \cos^2(qx) + \delta q \sin(qx) ] \psi_- &= E^2 \psi_-. \end{aligned} \quad (13)$$

It is sufficient to solve one of these equations, say, for  $\psi_+$ , since  $\psi_-$  is related to  $\psi_+$  by

$$\psi_-(x) = \frac{i}{E} \left[ -\partial/\partial x + \delta \cos(qx) \right] \psi_+(x), \quad (14)$$

provided  $E \neq 0$ . The energy spectrum can be found by solving the time-independent equation

$$[ -\partial^2/\partial x^2 + \delta^2 \cos^2(qx) - \delta q \sin(qx) ] \psi_+ = E^2 \psi_+. \quad (15)$$

Eq. (15) has the form of a Schrödinger equation (with “energy”  $E^2$ ) in the presence of a periodic potential. The potential is similar but not identical to Mathieu’s equation<sup>10</sup>. We therefore again expect bands to form. To simplify the notation, let us shift  $x$  by  $\pi/2q$  and then scale it by a factor of  $q$  to make the period equal to  $2\pi$ . We then get

$$[ -\partial^2/\partial x^2 + \frac{\delta^2}{q^2} \sin^2 x - \frac{\delta}{q} \cos x ] \psi_+ = \frac{E^2}{q^2} \psi_+. \quad (16)$$

By Floquet's theorem<sup>10</sup>, the solutions must satisfy  $\psi_+(x + 2\pi) = e^{i\theta}\psi_+(x)$ , where  $\theta$  goes from 0 to  $\pm\pi$  from the bottom of a band to the top. We observe that there is an exact zero energy state with  $\psi_+(x) = \exp(\frac{\delta}{q} \cos x)$  and  $\psi_-(x) = 0$  for which  $\theta = 0$ . In general, the nonzero energy states can only be found numerically. But if  $q/\delta$  is large, the positions of the low-lying bands (with  $E^2/q^2 \ll \delta/q$ ) can be found analytically as follows. For energies much lower than the maxima of the potential, we can ignore tunneling between the different wells to begin with. We note that there are two kinds of wells in Eq. (16); those centered about  $x = 2m\pi$  and those centered about  $x = (2m+1)\pi$ , where  $m$  can be any integer; the former wells are deeper than the latter. However, the *perturbative* energy levels (i.e., ignoring tunneling) are identical in the two types of wells, except for the  $E = 0$  state which only exists in the deeper wells. This identity follows from Eqs. (13) and (14) which show that corresponding to any (nonzero) energy eigenstate  $\psi_+(x)$  which lies in a deeper well, there is an eigenstate  $\psi_-(x)$  which lies in a shallower well. The  $n^{\text{th}}$  energy level in a deeper well has the same value as the  $(n-1)^{\text{th}}$  energy level in a shallower well, for  $n \geq 1$ . (This is an example of supersymmetric quantum mechanics<sup>11</sup>). It is therefore sufficient to find the energy levels of (16) which lie in one of the deeper wells, say, at  $x = 0$ . Near the bottom of that well, we have a simple harmonic potential with small anharmonic corrections. Ignoring the anharmonic terms, we find the energy levels to be simply given by

$$E_n^2 = 2nq\delta, \quad (17)$$

where  $n = 0, 1, 2, \dots$ . Next, we include the anharmonic corrections perturbatively. Up to second-order in perturbation theory, we get the more accurate expression

$$E_n = \sqrt{2nq\delta} \left[ 1 - \frac{n}{8} \frac{q}{\delta} - \frac{5n^2 + 2}{128} \frac{q^2}{\delta^2} \right]. \quad (18)$$

In Fig. 2, we show the six curves corresponding to  $n = 1$  to 6 in Eq. (18); for  $n = 0$ , we simply get a straight line lying at zero energy. We see that all the curves agree extremely well with the numerical data, even up to  $E_n$  of the order of  $\delta$  where the harmonic approximation breaks down and the band widths become noticeable.

We will now consider tunneling between wells using the WKB method. For  $n \ll \delta/q$ , the energy levels  $E_n^2/q^2$  of (16) lie in small intervals centered about  $x = m\pi$ , where  $m$  can be any integer for  $n \geq 1$  but must be an even integer for the  $n = 0$  band. In these small intervals, the potential is simple harmonic to a good approximation, with the harmonic frequency being equal to

$$b \equiv \delta/q. \quad (19)$$

We will assume that  $b$  is large so that the band widths are small. The splitting of the  $n^{\text{th}}$  band is given by the expression<sup>12</sup>

$$\begin{aligned} \frac{\Delta(E_n^2)}{q^2} &= \frac{4b}{\pi} \exp\left( - \int_{x_1}^{x_2} dx \sqrt{V(x) - 2nb} \right), \\ V(x) &= b^2 \sin^2 x - b \cos x, \end{aligned} \quad (20)$$

where  $x_1$  and  $x_2$  are the turning points, and we have approximated  $E_n^2/q^2$  by the lowest order result  $2nb$  given in (17). For  $n \geq 1$ , we take the turning points to be  $x_1 \simeq \sqrt{(2n+1)/b}$  and  $x_2 \simeq \pi - \sqrt{(2n-1)/b}$ , while for  $n = 0$ ,  $x_1 \simeq 1/\sqrt{b}$  and  $x_2 \simeq 2\pi - 1/\sqrt{b}$ . To lowest approximation, the exponential factor in (20) is given by  $\exp(-2b)$  for  $n \geq 1$  and by  $\exp(-4b)$  for  $n = 0$ . However, since  $\Delta(E_n^2) \simeq 2E_n\Delta E_n$  for a small width  $\Delta E_n$  if  $n \geq 1$ , but  $\Delta(E_0^2) = (\Delta E_0)^2$  (since  $E_0 = 0$ ), we see that the splitting  $\Delta E_n/q \sim \exp(-2b)$  for *all*  $n$ . We can do a more accurate calculation to find the prefactors; we find that

$$\frac{\Delta E_n}{\delta} \sim \frac{2^{3n+1}}{n! \sqrt{\pi}} \left( \frac{\delta}{q} \right)^{n-1/2} \exp\left( - \frac{2\delta}{q} \right) \quad (21)$$

for all values of  $n$ . We should note that the expression in (21) for  $n = 0$  actually gives *half* the width of that band since the  $n = 0$  band extends an equal amount to negative values of energy.

Eq. (21) explains why, with a numerical method using a finite energy resolution  $dE$ , the bands rapidly become thin and shrink to isolated points as  $q \rightarrow 0$  in Fig. 2. In Fig. 3, we compare the numerically obtained widths of the lowest four bands ( $n = 0, 1, 2, 3$ ) with the WKB expressions in (21). The points in that figure indicate the thirty smallest values of width that we could find using the condition  $|\text{tr } M(q, E)| \leq 2$  with the energy resolution  $dE = 10^{-6}$ ; the solid lines indicate the WKB expressions. We see that the agreement between the two becomes worse as  $q/\delta$  increases, particularly for the larger values of  $n$ . This is expected because the WKB method is accurate only if  $n \ll \delta/q$ .

We will now prove that the number of states lying below the line  $E/\delta = 1$  is proportional to  $\delta$ . For large  $\delta/q$ , we can use a semiclassical phase space argument to count how many states lie below any given energy. The ‘‘Hamiltonian’’ on the left hand side of Eq. (15) has the form  $p^2 + V(x)$ , where  $V(x) = \delta^2 \cos^2(qx) - \delta q \sin(qx)$ . Hence the number of states up to energy  $E$  is given by the phase space integral

$$\nu(E) = \frac{1}{L} \int \int \frac{dx dp}{2\pi} \Theta(E^2 - p^2 - V(x)), \quad (22)$$

where we have divided by the length  $L$  of the system for normalization; the  $\Theta$ -function is defined to be 1 and 0 if its argument is positive and negative, respectively. On doing the momentum integral in (22), we get

$$\nu(E) = \frac{q}{2\pi^2} \int_0^{2\pi/q} dx \sqrt{E^2 - V(x)} \Theta(E^2 - V(x)), \quad (23)$$

where we have used the fact that  $V(x)$  has period  $2\pi/q$ . For small values of  $q/\delta$ , we then see that the number of states lying between  $E = 0$  and  $\delta$  is

$$\nu(\delta) = \frac{2\delta}{\pi^2}, \quad (24)$$

which is *independent* of  $q$ . Incidentally, this also yields the number of bands lying below  $E = \delta$ . Since each band contains  $q/\pi$  states, Eq. (24) gives the number of bands to be  $2\delta/\pi q$ . We have verified that this estimate agrees very well with our numerical results.

We can obtain the density of states  $\rho(E)$  from the expression in (23) by differentiating it with respect to  $E$ . In the limit  $q/\delta \rightarrow 0$ , we get

$$\rho(E) = \frac{2}{\pi^2} \int_0^U d\eta \left[ 1 - \left( \frac{\delta}{E} \right)^2 \sin^2 \eta \right]^{-1/2},$$

where  $U = \sin^{-1}(E/\delta)$  if  $E < \delta$  and  $\pi/2$  if  $E > \delta$ . (25)

These are shown by the solid lines in Fig. 4; note the linear behavior near  $E/\delta = 0$  and the logarithmic divergence as  $E \rightarrow \delta$  from either side. This is to be contrasted with the density of states found exactly at  $q = 0$ . In that case,  $\rho(E)$  vanishes for  $E < \delta$  and is equal to  $1/[\pi\sqrt{1 - (\delta/E)^2}]$  for  $E > \delta$ . This is shown by the dashed line in Fig. 4.

The difference in the spectrum for  $q = 0$  and  $q \rightarrow 0$  should show up most clearly in the specific heat at temperatures  $T \ll \delta$ . Since the chemical potential is zero, the free energy per site is given by

$$F = -2T \int_0^\infty dE \rho(E) \ln(1 + e^{-E/T}), \quad (26)$$

The factor of 2 on the right hand side is because we have to sum over both fermions and holes which have the same density of states. (We set the Boltzmann constant equal to 1 for convenience). Then the specific heat per site is

$$C_V = - T \frac{\partial^2 F}{\partial T^2}. \quad (27)$$

For  $q = 0$ , the energy gap from  $-\delta$  to  $+\delta$  means that the specific heat vanishes exponentially at low temperature. But for  $q \rightarrow 0$ , Eq. (25) shows that the density of states goes linearly as  $\rho(E) \simeq E/(\pi\delta)$  for  $E \ll \delta$ . This implies that the low-temperature specific heat goes as  $T^2/\delta$  which is very different from the exponential behavior at  $q = 0$ .

We would like to point out here that the above results remain unchanged if the incommensurate term is present in the chemical potential  $\mu$  rather than in the hopping  $J_n$  in Eq. (1), provided that  $\delta$  and  $q$  are both *small*. In other words, if we start with the Hamiltonian

$$H = - \frac{1}{2} \sum_n ( c_n^\dagger c_{n+1} + c_{n+1}^\dagger c_n ) - \delta \cos(\pi + q)n \sum_n c_n^\dagger c_n, \quad (28)$$

we get the same continuum theory as discussed above, if we define the Fermi fields as in Eq. (11), followed by a phase redefinition  $\psi_L \rightarrow i\psi_L$ . This equivalence between the two continuum theories will be used below.

### C. Reconciling $q = 0$ with $q \rightarrow 0$ : the Azbel-Hofstadter problem

Let us ask: why does the model in Eq. (1) show such different behaviors in the limit  $q \rightarrow 0$  and at  $q = 0$ ? To answer this question, it is useful to generalize the form of the incommensurate hopping in (1) from  $\delta \cos(\pi + q)n$  to  $\delta \cos[(\pi + q)n + \eta]$ , where  $\eta$  is a phase lying between 0 and  $2\pi$ . If  $q/\pi$  is *irrational* (this is the generic case to consider if  $q$  is nonzero), the spectrum does not depend on  $\eta$ . [If  $q/\pi = M/N$  is rational, the spectrum does depend on  $\eta$ , but it varies less and less with  $\eta$  as  $N \rightarrow \infty$ . In our numerical computations, we introduced a random phase  $\eta$  for each value of  $q$  and found that this had no noticeable effect on the two figures]. This insensitivity to  $\eta$  can also be seen from the continuum theory in Eq. (12) where a potential of the form  $\cos(qx + \eta)$  can be transformed to  $\cos(qx)$  by shifting  $x$  appropriately. However, *exactly* at  $q = 0$ , the hopping has a term like  $\delta \cos \eta \cos(\pi n)$  and the spectrum depends significantly on  $\eta$ ; for instance, there is a gap from  $E = 0$  up to  $|\delta \cos \eta|$ , and the number of states up to an energy  $E$  is given by

$$\nu(E, \eta) = \frac{1}{\pi} \sqrt{E^2 - \delta^2 \cos^2 \eta} \quad (29)$$

for  $|\delta \cos \eta| < E \ll 1$ . We may now consider taking an *average* of this number over all possible values of  $\eta$ . Thus, the number of states up energy  $E$  is given by Eq. (29) to be

$$\nu(E) = \int_0^{2\pi} \frac{d\eta}{2\pi^2} \sqrt{E^2 - \delta^2 \cos^2 \eta} \Theta(E^2 - \delta^2 \cos^2 \eta). \quad (30)$$

This agrees with (23) if we substitute  $\eta = qx$ . Thus, the limit  $q \rightarrow 0$  agrees with the point  $q = 0$  *provided* that we average over  $\eta$  in the latter case.

The question now arises: is there a physical system where an average over the phase  $\eta$  occurs naturally? Some experimental systems sitting at  $q = 0$  (the dimerized point) are more likely to choose a particular value of  $\delta$  with  $\eta = 0$ , rather than average over many values of  $\eta$ ; the limit  $q \rightarrow 0$  and  $q$  exactly equal to



zero will therefore differ from each other. For simplicity, we will choose  $\eta = 0$  in the following sections to describe such systems.

There is, however, a problem in *two* dimensions which averages over  $\eta$  in a natural way. This is the Azbel-Hofstadter (AH) problem in which electrons hop on a regular lattice in the presence of an uniform magnetic field pointing normal to the plane. Let us consider a square lattice with the sites being labeled by two integers  $(m, n)$ . (We set the lattice spacing equal to 1 as usual). The hopping element from the site  $(m, n)$  to the site  $(m+1, n)$  will be denoted by  $t(m, n; \hat{x})$ , while hopping from  $(m, n)$  to  $(m, n+1)$  will be denoted by  $t(m, n; \hat{y})$ ; these will be complex numbers in general. Suppose that the hopping elements are all real in the absence of a magnetic field, with  $t(m, n; \hat{x}) = t_1$  and  $t(m, n; \hat{y}) = t_2$ . In the presence of a magnetic field, let  $\Phi$  denote the magnetic flux through each square. Then some of the hopping elements must necessarily be taken to be complex, with the sum of the phases of the four hopping elements taken anticlockwise around each square being equal to  $Q = e\Phi/(\hbar c)$ , where  $e$  is the electronic charge and  $c$  is the speed of light. We can interpret  $Q/(2\pi)$  as the ratio of the flux through each square to the flux quantum  $\Phi_0 = 2\pi\hbar c/e$ . Clearly,  $Q$  and  $Q + 2\pi$  are physically indistinguishable; thus,  $Q = \pi$  corresponds to the largest magnetic field that can appear on a lattice. Now, there are many choices possible for distributing the phases amongst the different hopping elements; the different choices are related to each other by gauge transformations. Let us choose the Landau gauge in which the hopping elements in the  $\hat{y}$  direction stay real and are equal to  $t_2$ , while the hopping elements in the  $\hat{x}$  direction are given by

$$t(m, n; \hat{x}) = t_1 \exp(-iQn) . \quad (31)$$

The lattice Schrödinger equation satisfied by the single-particle wave functions is then given by

$$t_1 ( \exp(iQn) \phi_{m+1, n} + \exp(-iQn) \phi_{m-1, n} ) + t_2 ( \phi_{m, n+1} + \phi_{m, n-1} ) = e \phi_{m, n} . \quad (32)$$

Since the hopping elements do not depend on the  $\hat{x}$ -coordinate  $m$ , we may assume the wave functions to have the factorized form

$$\phi_{m, n} = \exp(im\eta) \psi_n , \quad (33)$$

where the momentum  $\eta$  can take any value from 0 to  $2\pi$ . Eq. (32) then takes the form

$$-\frac{1}{2} ( \psi_{n+1} + \psi_{n-1} ) - \frac{t_1}{t_2} \cos(Qn + \eta) \psi_n = -\frac{e}{2t_2} \psi_n . \quad (34)$$

This is the well-studied Harper's equation with an on-site incommensurate term. Further, we see that a phase  $\eta$  appears naturally in that term, and that we have to consider all values of  $\eta$  lying in the interval  $[0, 2\pi]$ .

Let us consider the extremely anisotropic limit  $\delta \equiv t_1/t_2 \ll 1$ . We will show that this problem has the same continuum limit as the problem in which the incommensurate term is in the hopping. If we define

$$\delta = \frac{t_1}{t_2} \quad \text{and} \quad E = -\frac{e}{2t_2} , \quad (35)$$

then the Hamiltonian corresponding to Eq. (34) can be written as  $H = H_0 + V_\delta$ , where the incommensurate term is

$$V_\delta = -\delta \sum_n \cos(Qn + \eta) c_n^\dagger c_n . \quad (36)$$

The matrix elements of  $V_\delta$  between momentum eigenstates of  $H_0$  are given by

$$\langle k_1 | V_\delta | k_2 \rangle = - \frac{\delta}{2} ( \delta_{Q+k_1, k_2} e^{-i\eta} + \delta_{Q+k_2, k_1} e^{i\eta} ) . \quad (37)$$

For  $Q$  close to  $\pi$  and  $k_1, k_2$  close to  $\pm\pi/2$ , this has, up to factors of  $i$ , the same form as (8), except that we have to average over  $\eta$  in the AH problem. We thus see that the anisotropic limit of the AH problem provides us with a physical realization of Eq. (1) except that we have to consider a phase average of the incommensurate term. Dimerization in the one-dimensional problem corresponds to  $Q = \pi$ , namely, the magnetic flux through each square of the two-dimensional lattice is equal to half a flux quantum. We may therefore carry over all our results to that particular limit of the AH problem. For instance, the density of states for  $Q \rightarrow \pi$  has the form given by the solid lines in Fig. 4. Note that the energy spectrum does not depend on the phase  $\eta$  for generic (i.e., irrational) values of  $Q$  in Eq. (34). So if  $L_x$  denotes the number of lattice sites in the  $\hat{x}$ -direction, the number of values of  $\eta$  is also equal to  $L_x$  since  $\eta$  takes all values from 0 to  $2\pi$  in steps of  $2\pi/L_x$ . Hence the density of states for the AH problem is equal to  $L_x$  times the density given in Fig. 4 for the one-dimensional problem.

We note that the energy eigenvalues in Eq. (32) are invariant under the exchange  $t_1 \leftrightarrow t_2$  corresponding to an interchange of the  $\hat{x}$  and  $\hat{y}$  hopping elements in the Landau gauge. Thus the AH problem has the duality symmetry  $\delta \rightarrow 1/\delta$ . Our problem with an incommensurate hopping has no such symmetry.

With the present day expertise in fabricating quantum dot arrays, it may be possible to construct a two-dimensional lattice whose spacing is large enough that the flux through each square could be made equal to half a flux quantum with currently available magnetic field strengths. (A similar suggestion was made by Hofstadter<sup>7</sup>). Consequently, our expression for the density of states of such a system could be experimentally tested.

### III. INTERACTING FERMIONS CLOSE TO DIMERIZATION

Let us now return to one dimension. In this section, we will argue that the difference between small  $q$  and  $q = 0$  (in particular, the presence of states within the  $q = 0$  gap) persists for the more interesting case of interacting fermions, i.e., for Luttinger liquids. To this end, consider adding a four-fermion interaction term like  $\sum_n c_n^\dagger c_n c_{n+1}^\dagger c_{n+1}$  to the Hamiltonian (1). Equivalently, we can consider an  $XXZ$  spin-1/2 chain governed by

$$H = \sum_n \left[ ( 1 + \delta \cos(\pi + q)n ) ( S_n^x S_{n+1}^x + S_n^y S_{n+1}^y ) + D S_n^z S_{n+1}^z \right] . \quad (38)$$

which is related to the interacting fermion theory by a Jordan-Wigner transformation<sup>13</sup>. If the incommensurate term is absent ( $\delta = 0$ ), it is known from the exact Bethe ansatz solution and conformal field theory<sup>14</sup> that the model in (38) is gapless with a linear dispersion of the low-energy excitations if  $-1 < D \leq 1$ . If we now add a dimerization ( $q = 0$  and  $\delta$  is small), then the system becomes gapped and the gap scales as

$$\Delta E = \delta^{1/(2-K)} ,$$

where  $K = \frac{\pi}{2 \cos^{-1}(-D)} ,$  (39)

where  $0 < \cos^{-1}(-D) \leq \pi$ . [Actually, a gap opens up only if  $K \leq 2$ . If  $K > 2$ , the dimerization term is irrelevant in the sense of the renormalization group, and a gap is not generated]. It is useful to state the result in Eq. (39) in the language of bosonization. We introduce a bosonic field  $\phi(x, t)$  such that bilinears in Fermi fields have local expressions in terms of the bosonic field<sup>14</sup>. For instance,

$$\begin{aligned} \psi_R^\dagger \psi_L &\sim \exp(i2\phi) , \\ \psi_L^\dagger \psi_R &\sim \exp(-i2\phi) , \end{aligned} \quad (40)$$

and

$$\partial\phi/\partial x = -\pi [\rho(x) - \rho_0], \quad (41)$$

where  $\rho(x)$  is the local fermion density, and  $\rho_0$  is the average density. For  $q = 0$ , the model in (38) is equivalent, at low energies, to a sine-Gordon theory described by the Lagrangian density<sup>14</sup>

$$\mathcal{L} = \frac{1}{2\pi v K} \left[ (\partial\phi/\partial t)^2 - v^2 (\partial\phi/\partial x)^2 \right] - \alpha \delta^{2/(2-K)} [1 - \cos(2\phi)], \quad (42)$$

where  $v$  is the velocity of low-energy excitations and  $\alpha$  is a positive constant; their numerical values are not important here. The main point is to note the exponent of  $\delta$  in the coefficient of  $\cos(2\phi)$ . (There are also factors of  $\ln \delta$  due to the presence of a marginal operator in the  $XXZ$  model<sup>15</sup>, but we will ignore such terms here). The number  $K$  and the velocity  $v$  are the two important parameters which determine the low-energy, long wavelength behavior of a Luttinger liquid.

It is important to observe that the incommensurate term which is *linear* in  $\delta$  in the original fermionic theory in (38) becomes a cosine term with a different exponent for  $\delta$  in the low-energy bosonic theory. This is because a nontrivial renormalization occurs in the process of deriving the low-energy bosonic theory from the microscopic fermionic theory<sup>8,16</sup>. This renormalization occurs even if the fermions are noninteracting, i.e., for the  $XY$  spin-1/2 chain with  $D = 0$  in (38) and  $K = 1$ ; the reason for this is that the sine-Gordon theory is always strongly interacting. These strong interactions are also responsible for the large renormalizations of the correct quantum spectrum compared to the naive (i.e. classical) spectrum that one obtains from the sine-Gordon theory, namely, the classical soliton mass for the fermionic excitations and the quadratic fluctuations around  $\phi = 0$  spectrum for the bosonic excitations<sup>17</sup>. The noninteracting fermionic model in (1) has no such renormalizations, which is why we did not use bosonization in the earlier part of this paper.

Let us now change  $q$  slightly away from zero. Since  $\cos(\pi + q)n = \cos(\pi n)\cos(qn)$  on a lattice, we have a dimerization whose coefficient  $\delta \cos qn$  varies very slowly over the system. Thus, the low-energy excitations, which had a relativistic dispersion with the mass  $\delta^{1/(2-K)}$  for  $q = 0$ , now have a space-dependent mass  $|\delta \cos(qx)|^{1/(2-K)}$ . To put it differently, bosonization yields a theory of the sine-Gordon type, except that the coefficient of the  $\cos(2\phi)$  term in Eq. (42) gets modified to produce

$$\mathcal{L} = \frac{1}{2\pi v K} \left[ (\partial\phi/\partial t)^2 - v^2 (\partial\phi/\partial x)^2 \right] - \alpha |\delta \cos(qx)|^{2/(2-K)} [1 - \cos(2\phi)], \quad (43)$$

Unlike (42), the theory in Eq. (43) cannot be solved analytically, either in classical or in quantum mechanics. However we can make some qualitative statements about the low-energy spectrum if  $q/\delta \ll 1$ . When calculating the spectrum of small oscillations about a classical ground state  $\phi = 0$ , we find it convenient to first shift  $x$  by  $\pi/(2q)$  to change  $\cos(qx)$  to  $\sin(qx)$ , and to then scale  $x$  by a factor of

$$a = (q\delta)^{1/(3-K)}. \quad (44)$$

This gives the eigenvalue equation

$$-v^2 \frac{\partial^2 \phi}{\partial x^2} + 4\pi K \alpha v |x|^{2/(2-K)} \phi = \left(\frac{E}{a}\right)^2 \phi \quad (45)$$

for eigenstates lying close to the origin  $x = 0$ ; we have approximated  $\sin(qx)$  by  $qx$  and  $\sin(2\phi)$  by  $2\phi$ . Since (45) is the Schrödinger equation with a confining potential, we see that the energy can take several discrete values which are given by numerical factors multiplying  $a$ . [Note that our earlier results for noninteracting fermions agree with this scaling argument if we set  $K = 1$ ]. These discrete values will then spread out into bands once we include tunneling between the different wells centered at the points

$x = m\pi$ . Similarly, we can find the energy of a classical soliton which goes from  $\phi = 0$  at  $x \rightarrow -\infty$  to  $\phi = \pi$  at  $x \rightarrow \infty$ ; once again we can show by scaling that this will be given by  $a$  times some numerical factor. [Of course, all the numerical factors will get renormalized due to quantum corrections, but the power-law dependence on  $q\delta$  is not expected to change]. We therefore see that all the low-lying excitations have energies of the order of  $(q\delta)^{1/(3-K)}$ ; this is much smaller than the gap which exists exactly at  $q = 0$  given by Eq. (39), since we are assuming that  $q/\delta$  is small. We thus see that in the limit  $q \rightarrow 0$ , there are many states which lie within that gap. Indeed, we can use WKB quantization for Eq. (45) to estimate that the number of bands lying between zero energy and the gap  $\Delta E$  in (39) is of the order of  $\Delta E/q$ , in the limit  $q \rightarrow 0$ . The number of states in the same interval is therefore of the order of  $\Delta E$ ; this also follows from the semiclassical argument presented below.

The semiclassical phase space estimate given in Eq. (23) can be used to find the density of states  $\rho(E)$  at energies much smaller than the  $q = 0$  gap. If  $E \ll \delta^{1/(2-K)}$ , the wave function for that state lies in a region where we can approximate  $\sin(qx)$  by  $qx$ . Ignoring various numerical factors, we then get

$$\rho(E) = \frac{d}{dE} \int_0^{2\pi/q} \frac{qdx}{\pi} \sqrt{E^2 - (\delta qx)^{2/(2-K)}} \Theta(E^2 - (\delta qx)^{2/(2-K)}) \sim \frac{E^{2-K}}{\delta}. \quad (46)$$

Since the chemical potential for these bosonic excitations is zero, the free energy per site is given by

$$F = T \int_0^\infty dE \rho(E) \ln(1 - e^{-E/T}). \quad (47)$$

The specific heat at temperatures much lower than the  $q = 0$  gap therefore scales as  $T^{3-K}/\delta$ , which is again much larger than the exponential dependence which occurs at  $q = 0$ . [It is tempting to compare this exponential versus power-law dependence of the specific heat with the forms of the specific heats of the magnetic excitations observed in the dimerized ( $q = 0$ ) and incommensurate ( $q \neq 0$ ) phases of  $CuGeO_3$ <sup>6</sup>. However that system is much more complicated because it has strong phonon-spin couplings; we have ignored such terms in our model by assuming that the incommensuration is static].

We should note that Eq. (23) counts the number of one-particle fermionic states, and the specific heat calculated from that gets a contribution from states with all possible fermion numbers. Eq. (46), however, only counts the number of one-particle bosonic states, i.e., fermion-hole excitations. Hence the specific heat calculated from that only gets a contribution from states with zero fermion number. However the complete expression for the specific heat is expected to differ only by numerical factors from the bosonic one, and should therefore have the same kind of exponential or power-law dependence on the temperature.

#### IV. FERMIONS NEAR OTHER COMMENSURATE FILLINGS

It is interesting to note that the peculiar difference between the limit  $q \rightarrow 0$  and  $q = 0$  only occurs near dimerization, i.e., near wave number  $\pi$ . There is no such singularity at  $q = 0$  if we take the incommensurate term in Eq. (1) to be of the form  $\delta \cos(Qn)$ , where  $Q = Q_0 + q$  and  $Q_0/\pi$  is equal to some simple rational number *different* from 1. Let us first see this for the case of noninteracting fermions. Imagine filling up the Fermi sea up to a Fermi energy  $E_F = -\cos k_F$  where  $k_F = Q_0/2$ ; the Fermi velocity is then  $v = \sin k_F$ . We define the continuum Dirac field as

$$\psi(x) = \psi_R(x) \exp(ik_F x) + \psi_L(x) \exp(-ik_F x), \quad (48)$$

After dropping terms like  $\exp(\pm ik_F x)$  which vary rapidly, the Dirac equations take the form

$$\begin{aligned}
i \left( \partial/\partial t + v\partial/\partial x \right) \psi_R + \frac{\delta}{2} \exp(iqx - ik_F) \psi_L &= 0, \\
i \left( \partial/\partial t - v\partial/\partial x \right) \psi_L + \frac{\delta}{2} \exp(-iqx + ik_F) \psi_R &= 0.
\end{aligned} \tag{49}$$

The solutions of this equation have the plane wave form

$$\begin{pmatrix} \psi_R(x, t) \\ \psi_L(x, t) \end{pmatrix} = \exp(-iEt) \begin{pmatrix} a_R \exp(ikx + iqx/2 - ik_F/2) \\ a_L \exp(ikx - iqx/2 + ik_F/2) \end{pmatrix}. \tag{50}$$

On substituting this in (49), we find that there is a single energy gap lying between  $E_+$  and  $E_-$  given by

$$E_{\pm} = \frac{1}{2} ( vq \pm \delta ). \tag{51}$$

Thus the size of the gap,  $\delta$ , is independent of  $q$ . (All these calculations assume that  $q$  and  $\delta$  are both small; the gap size may depend on  $q$  if  $q$  is not small). If  $\delta$  is held fixed and  $q$  is increased from zero, a state first appears at zero energy when  $q$  reaches the value  $\delta/v$ . It is instructive to express all this in the language of bosonization. Since  $K = 1$ , we can combine Eqs. (40) and (49) to show that the sine-Gordon Lagrangian takes the form

$$\mathcal{L} = \frac{1}{2\pi v} \left[ (\partial\phi/\partial t)^2 - v^2 (\partial\phi/\partial x)^2 \right] - \frac{\pi\delta^2}{16v} [ 1 - \cos(2\phi + qx - k_F) ]. \tag{52}$$

Note that we have fixed the coefficient of  $\cos(2\phi)$  in such a way that, for  $q = 0$ , the soliton mass, including the quantum corrections<sup>17</sup>, is exactly equal to the gap from zero energy, i.e.,  $\delta/2$ . On shifting  $\phi$  by  $(qx - k_F)/2$ , we get

$$\mathcal{L} = \frac{1}{2\pi v} \left[ (\partial\phi/\partial t)^2 - v^2 (\partial\phi/\partial x - q/2)^2 \right] - \frac{\pi\delta^2}{16v} [ 1 - \cos(2\phi) ]. \tag{53}$$

The Hamiltonian therefore contains a boundary term

$$H_b = - \frac{qv}{2\pi} [ \phi(\infty) - \phi(-\infty) ] \tag{54}$$

which is purely topological; it is equal to  $-qv/2$  in a one-soliton state. We thus see that if  $q$  is increased from zero, the energy of the one-soliton state becomes equal to that of the ground state (whose soliton number is zero) when  $q$  reaches the value  $\delta/v$ . From (41), we observe that a soliton corresponds to a hole; thus the energy of a hole (i.e., the energy required to remove one fermion from the system) becomes zero at  $q = \delta/v$ . Conversely, the energy required to add a fermion (antisoliton) to the system becomes zero at  $q = -\delta/v$ . [Similar results appear in the context of incommensurate crystals<sup>4,8,9</sup>].

To illustrate these results, we show the two major bands and the big gap separating them near the wave number  $Q_0 = 2\pi/3$  and the Fermi energy  $E_F = -\cos(\pi/3) = -1/2$  in Fig. 5; we have taken  $\delta = 0.4$ . [We have chosen a bigger value of  $\delta$  here compared to Figs. 1 and 2 in order to discuss some additional gaps in Sec. V and Fig. 6 below; those small gaps would not have been visible in Fig. 5 if we had chosen values of  $\delta$  much less than 0.4]. We used the condition  $\text{tr } M(q, E) \leq 2$  to find the energy levels, and we used the energy resolution  $dE = 10^{-5}$ . Note that the upper and lower edges of the gap follow Eq. (51), and the gap closes with respect to  $E_F$  at  $q/\delta = \pm 1/v$ , where  $1/v = 2/\sqrt{3} = 1.1547\dots$ . It is remarkable how simple Fig. 5 is compared to Figs. 1 and 2.

Thus, if  $Q_0 \neq \pi$ , there is a critical and nonzero value of  $q$  at which the gap closes at zero energy. This is very different from the earlier case with  $Q_0 = \pi$ , where there is always a band of energies lying around

zero energy, so that there is no gap at zero energy for any  $q \neq 0$ . (Our results disagree with Ref. 8 which argues that there is a nonzero critical value of  $q$  for  $Q_0 = \pi$ ).

Finally, we can show that there is a nonzero critical value of  $q$  where the gap closes if  $Q \neq \pi$  and the fermions are *interacting*. By following arguments similar to the ones above, we find that the continuum theory is described by a combination of the Lagrangian in (42) (for  $q = 0$ ) and the boundary term in (54) (for  $q$  nonzero but small). The soliton gap for  $q = 0$  is given by  $\Delta E \sim \delta^{1/(2-K)}$ ; hence the boundary term implies that the soliton (antisoliton) gap will become zero at  $q = \pm q_c$  where

$$q_c = \frac{2K\Delta E}{v}. \quad (55)$$

We thus get an expression for the critical value of  $q$  in terms of the  $q = 0$  gap and the two Luttinger parameters  $K$  and  $v$ .

## V. HIGHER ORDER CONTINUUM THEORIES FOR NONINTERACTING FERMIONS WITH INCOMMENSURATE HOPPING

In this section, we will consider the complete energy spectrum of noninteracting fermions with a weak incommensurate hopping. (This will complement the pictures of the complete spectrum of noninteracting fermions with an incommensurate on-site potential given in the works of Hofstadter and of Sun and Ralston<sup>7</sup>). In contrast to Secs. II and IV, we will use continuum theories which go up to higher than linear order in  $\delta$ . This will enable us to look at some of the smaller gaps in the energy spectrum as can be seen in Fig. 7.

The basic point is the following. Suppose that the incommensurate term  $V_\delta$  has Fourier components at wave numbers  $\pm Q$  (where  $Q = Q_0 + q$ ), and that we are interested in the vicinity of the two Fermi points at momenta  $\pm k_F$ . (We assume that  $0 < Q_0 < 2\pi$  and  $0 < k_F < \pi$ ). Then a gap develops at the Fermi points if there exists an integer  $m$  (positive or negative) such that

$$-k_F + mQ_0 = k_F \pmod{2\pi}. \quad (56)$$

To lowest order in the strength of the incommensuration  $\delta$ , the gap at the Fermi points is of order  $\delta^{|m|}$ , since  $V_\delta$  must act  $|m|$  times to take us from the momentum state  $-k_F$  to  $k_F$  or vice versa. Now suppose that there is another integer  $n$  such that

$$-k_F + nQ_0 = k_F \pmod{2\pi}. \quad (57)$$

We now have the possibility of interference between the actions of  $V_\delta^{|m|}$  and  $V_\delta^{|n|}$ , i.e. between terms in the continuum theory of the forms  $\delta^{|m|}e^{imqx}$  and  $\delta^{|n|}e^{inqx}$ . This interference gives rise to a large number of gaps and bands as we can show through a harmonic potential approximation. It is clear that conditions (56) and (57) can hold simultaneously only if  $Q_0/\pi$  and  $k_F/\pi$  are rational numbers.

There are now two possibilities which we will call A and B. In case A,  $m = -n$ , which necessarily means that  $k_F = \pi/2$  and  $E_F = 0$ . In that case, all the gaps are of the order  $\delta^{|m|}$ . The discussion in Sec. II B and Figs. 1 and 2 is an example of case A, with  $Q_0 = \pi$ ,  $k_F = \pi/2$  and  $m = -n = 1$ . In case B,  $|m| < |n|$ . Here, there is one big gap of order  $\delta^{|m|}$  and all the other gaps are of order  $\delta^{|n|}$ .

As an example of case B, let us consider the two small gaps originating from the top and bottom of the big gap shown in Fig. 5 at  $q/\delta = 0$ . We will only discuss the gap at the top here. An enlargement of that region is shown in Fig. 6 where it is clear that there are actually several small bands and gaps emerging from the top of the big gap; only the largest of these small gaps is visible in Fig. 5. This region can be understood as follows. Following the notation in Eqs. (56-57), we have  $Q_0 = 2\pi/3$ ,  $k_F = \pi/3$ ,

$m = 1$  and  $n = -2$ . As discussed in Sec. IV, the effect of (56) is linear in  $\delta$ . We now have to consider the effect of (57) which is of second order in  $\delta$ . The fact that two applications of  $V_\delta$  can take us from the modes near  $-k_F$  to the modes near  $k_F$  has three different effects.

(i) At  $q = 0$ , it shifts the position of the lower edge of the upper band from the value  $E_{q=0} = E_F + E_+ = -1/2 + \delta/2$  given in Eq. (51) with  $E_F = -1/2$ . This shift can actually be calculated exactly, not just to order  $\delta^2$ , by considering the three states with momenta  $-\pi/3, \pi/3$  and  $\pi$  and writing down the matrix elements of  $H_0 + V_\delta$  between these states as a  $3 \times 3$  matrix. One of the eigenvalues of this matrix gives the position of the lower edge of the upper band to be

$$E_{q=0} = \frac{1}{4} + \frac{\delta}{4} - \frac{1}{4} \left( 9 - 6\delta + 3\delta^2 \right)^{1/2}. \quad (58)$$

(ii) At second-order in  $V_\delta$ , we can go from the a state near  $-\pi/3$  to a state near  $\pi$  and then back to the original state near  $-\pi/3$ ; similarly, we can go from  $\pi/3$  to  $\pi$  and back to  $\pi/3$ . This changes the velocity  $v = \partial E / \partial k$  from  $v = \sqrt{3}/2$  to

$$v = \frac{\sqrt{3}}{2} \left( 1 - \frac{\delta^2}{36} \right). \quad (59)$$

(iii) Finally, we can define the continuum Dirac fields as in (48). After performing the transformation in (50) and shifting  $x$  by an appropriate amount, we get the time-independent equations

$$\begin{aligned} [\tilde{E} + iv\partial/\partial x] a_R + \frac{\delta}{2} \left[ 1 - \frac{\delta}{12} \exp(-i3qx) \right] a_L &= 0, \\ [\tilde{E} - iv\partial/\partial x] a_L + \frac{\delta}{2} \left[ 1 - \frac{\delta}{12} \exp(i3qx) \right] a_R &= 0, \end{aligned} \quad (60)$$

where

$$\begin{aligned} \tilde{E} &= E - \frac{vq}{2} - E_{q=0} + \beta, \\ \beta &= \frac{\delta}{2} \left( 1 - \frac{\delta}{12} \right). \end{aligned} \quad (61)$$

Thus we get a periodic potential as in Sec. II B. Following the procedure in that section, we first study the harmonic oscillator energies near the bottom of one of the wells, say, at  $x = 0$ ; then we will briefly comment on the broadening of those energies due to tunneling between different wells. On expanding  $\exp(\pm i3qx)$  up to order  $q^2$ , we find that the fields  $a_\pm = a_R \pm a_L$  satisfy the harmonic oscillator equations

$$\left[ -\frac{1}{2} \partial^2/\partial x^2 + \frac{1}{2} \omega^2 x^2 + \frac{\beta^2 - \tilde{E}^2}{2v^2} \right] a_\pm = 0, \quad (62)$$

where the harmonic frequency is

$$\omega = \frac{\sqrt{3}}{4} \frac{\delta^{3/2}|q|}{v}. \quad (63)$$

The harmonic approximation is good if the root mean square deviation of the particle  $\langle x^2 \rangle^{1/2} \sim 1/\sqrt{\omega}$  is much smaller than  $2\pi/3q$  which is the periodicity of the potential in (60). We therefore assume that

$$v |q| \ll \delta^{3/2}. \quad (64)$$

We then find the energy levels to be

$$E_n = E_{q=0} + \frac{vq}{2} - \beta + \left[ \beta^2 + 2v^2\omega(n + \frac{1}{2}) + \frac{vq\delta^2}{8} \right]^{1/2}, \quad (65)$$

where  $n \geq 0$ . The term  $vq\delta^2/8$  inside the square root comes from perturbatively including the first anharmonic correction. The eight solid lines in Fig. 6 show the energies in (65) for  $n = 0, 1, 2, 3$ , and for positive and negative values of  $q$ . The agreement is good for small values of  $q$ . We can now use the WKB approximation to study the band widths due to tunneling between wells; we find that the widths go as

$$\Delta E_n \sim \exp\left(-\frac{4}{9} \frac{\delta^{3/2}}{|q|}\right). \quad (66)$$

If  $\delta$  and  $q/\delta$  are both small, then (66) is much larger than the factor of  $\exp(-2\delta/q)$  obtained in Eq. (21). Qualitatively, this explains why the bands in Fig. 6 broaden much more rapidly than the ones in Fig. 2 as  $q$  increases from zero.

Fig. 7 shows the complete picture of bands and gaps for all values of  $Q$  with  $\delta = 0.4$ . We see that the gaps come in two classes. As discussed above, a gap arising from case B consists of a small gap (which, at higher resolution, is actually a group of bands and gaps) emerging from one point on one edge of a big gap. On the other hand, a gap arising from case A looks like a cross in which four groups of gaps meet at a point; this can be seen in Fig. 7 at  $E = 0$  and  $Q/\pi = 1/m$  where  $m = 1, 2, 3, \dots$ . The simplest example of this corresponds to  $m = 1$  which was discussed in Sec. II B.

Let us now consider higher values of  $m$ . In general, we can go from the states near  $-\pi/2$  to states near  $\pi/2$  in  $m$  steps, either through the intermediate states with increasing momenta at  $k_j = -\pi/2 + j\pi/m$  with  $j = 1, 2, \dots, m$ , or through the intermediate states with decreasing momenta at  $k_j = -\pi/2 - j\pi/m$  with  $j = 1, 2, \dots, m$ . In each case, we get a product of  $m$  matrix elements from (8) divided by  $m - 1$  energy factors like  $E_j - E_F$  where  $E_F = 0$ . To be explicit, this product is

$$F_m = (\delta/2)^m \frac{\prod_{p=0}^{m-1} \sin[(p + \frac{1}{2})\pi/n]}{\prod_{p=1}^{m-1} \sin[p\pi/m]} = \frac{\delta^m}{m 2^m}. \quad (67)$$

(The second equality follows from the identity

$$\prod_{p=1}^{n-1} [2 \sin(p\pi/n)] = \lim_{z \rightarrow 1} \prod_{p=1}^{n-1} (z - e^{i2\pi p/n}) = \lim_{z \rightarrow 1} \frac{z^n - 1}{z - 1} = n). \quad (68)$$

After adding the contributions from the two sets of intermediate states and shifting  $x$  appropriately, we get a term in the continuum Hamiltonian of the form

$$2F_m (\psi_R^\dagger \psi_L + \psi_L^\dagger \psi_R) \cos(mqx). \quad (69)$$

This gives rise to a Dirac equation whose form is identical to that in Eq. (12) except that  $q$  and  $\delta$  in that equation are now replaced by  $mq$  and

$$2F_m = \frac{\delta^m}{m 2^{m-1}} \quad (70)$$

respectively. We therefore get the same pattern of bands and gaps as in Figs. 1 and 2; we recall here that those figures only show one-fourth of the region of interest since they are restricted to positive values of  $q$  and  $E$ . The complete regions which resemble crosses are visible in Fig. 7 along the line  $E = 0$  at the



values  $Q/\pi = 1/m$ . The change of scale from  $\delta$  to  $2F_m$  in Eq. (70) explains why the sizes of the crosses decrease rapidly as  $m$  increases.

This concludes our discussion of the main features of the complete energy spectrum with incommensurate hopping. Due to the close relationship of our work with the anisotropic AH problem, it is not surprising that our Fig. 7 resembles the complete energy spectrum with an incommensurate on-site potential as given in, say, Fig. 7 of Sun and Ralston<sup>7</sup>. (Their variables  $\Phi/\Phi_0$  and  $\lambda$  correspond to our  $Q/(2\pi)$  and  $1/\delta$  respectively). For instance, their figure also shows a series of crosses along the line  $E = 0$ . Due to the differences in the matrix elements in (8) versus the ones in (37), the scales of the crosses go as

$$2F_m = \frac{\delta^m}{m} \quad (71)$$

for the case of on-site incommensuration. This decreases more slowly than (70) with increasing  $m$  which explains why the crosses in Sun and Ralston are bigger than the ones in our Fig. 7; they also have larger values of  $\delta$  equal to 1 and 2/3 compared to our  $\delta = 0.4$ . Similarly, their figure shows the smaller gaps on the edges of the larger gaps as explained by our case B.

## VI. OUTLOOK

The continuum method discussed in this paper is robust in the sense that it can be applied even if we add weak next-nearest-neighbor hoppings or the incommensuration is given by the sum of several harmonics. This is an advantage over some other analytical methods. For instance, the Bethe ansatz discussed by Wiegmann and Zabrodin<sup>7</sup> only works in somewhat special cases; in those cases, however, the Bethe ansatz works for all values of  $\delta$ . A limitation of the continuum method is that it is accurate only if the incommensuration is weak.

An interesting problem for future study may therefore be to examine what happens if the incommensuration in the hopping is strong, i.e., if  $\delta$  is comparable to or larger than 1. [Both the perturbative and the continuum Dirac theory (or bosonization) approaches would then fail. Further, for strong incommensuration, it does make a difference whether the incommensurate term is in the hopping or on-site; the latter case has been studied much more extensively in the literature]. The pattern of bands and gaps is expected to be much more complicated in that case, perhaps with a devil's staircase or a point spectrum structure<sup>1,3,4,7</sup>. The nature of the wave functions, namely, whether they remain extended or become localized, would also be of interest.

## Acknowledgments

We thank G. Ananthakrishna, Somen Bhattacharjee, Rahul Pandit and, specially, Apoorva Patel for many useful discussions.

- 
- <sup>1</sup> J. B. Sokoloff, Phys. Rep. **126**, 189 (1985); J. M. Luck, J. Stat. Phys. **72**, 417 (1993) and Phys. Rev. B **39**, 5834 (1989); J. Bellissard, in *From Number Theory to Physics*, edited by M. Waldschmidt, P. Moussa, J. M. Luck and C. Itzykson (Springer, Berlin, 1992).
- <sup>2</sup> M. C. Valsakumar and G. Ananthakrishna, J. Phys. C **20**, 9 (1987).
- <sup>3</sup> S. Ostlund and R. Pandit, Phys. Rev. B **29**, 1394 (1984).
- <sup>4</sup> I. Lyuksyutov, A. G. Naumovets and V. Pokrovsky, *Two-Dimensional Crystals* (Academic Press, San Diego, 1992); P. M. Chaikin and T. C. Lubensky, *Principles of condensed matter physics* (Cambridge University Press, Cambridge, 1998).
- <sup>5</sup> R. Merlin, K. Bajema, R. Clarke, F.-Y. Juang and P. K. Bhattacharya, Phys. Rev. Lett. **55**, 1768 (1985).
- <sup>6</sup> T. Lorenz *et al*, Phys. Rev. B **54**, 15610 (1996); J. P. Boucher and L. P. Regnault, J. de Phys. I **6**, 1939 (1996); G. S. Uhrig, preprint cond-mat/9904387.
- <sup>7</sup> M. Ya. Azbel, Sov. Phys. JETP **19**, 634 (1964); D. R. Hofstadter, Phys. Rev. B **14**, 2239 (1976); W. Y. Hsu and L. M. Falicov, Phys. Rev. B **13**, 1595 (1976); G. M. Obermair and H.-J. Schellnhuber, *ibid.* **23**, 5185 (1981); H.-J. Schellnhuber, G. M. Obermair and A. Rauh, *ibid.* **23**, 5191 (1981). S. N. Sun and J. P. Ralston, Phys. Rev. B **44**, 13603 (1991); P. B. Wiegmann and A. V. Zabrodin, Phys. Rev. Lett. **72**, 1890 (1994).
- <sup>8</sup> S. M. Bhattacharjee and S. Mukherji, J. Phys. A **31**, L695 (1998).
- <sup>9</sup> T. Nakano and H. Fukuyama, J. Phys. Soc. Jpn. **49**, 1679 (1980); *ibid.* **50**, 2489 (1981).
- <sup>10</sup> M. Abramowitz and I. A. Stegun, *Handbook of Mathematical Functions* (Dover Publications, New York, 1972).
- <sup>11</sup> E. Witten, Nucl. Phys. B **188** (1981) 513; R. Dutt, A. Khare and U. P. Sukhatme, Am. J. Phys. **56** (1988) 163.
- <sup>12</sup> D. ter Haar, *Problems in Quantum Mechanics* (Pion Ltd., London, 1975).
- <sup>13</sup> E. Lieb, T. Schultz and D. Mattis, Ann. Phys. (N. Y.) **16**, 407 (1961); P. Pfeuty, *ibid.* **57**, 79 (1970).
- <sup>14</sup> H. J. Schulz, G. Cuniberti and P. Pieri, Lecture Notes of the Chia Laguna summer school 1997, cond-mat/9807366; I. Affleck, in *Fields, Strings and Critical Phenomena*, edited by E. Brezin and J. Zinn-Justin (North-Holland, Amsterdam, 1989); F. D. M. Haldane, Phys. Rev. Lett. **50**, 1153 (1983) and Phys. Lett. **93A**, 464 (1983).
- <sup>15</sup> I. Affleck, D. Gepner, H. J. Schulz and T. Ziman, J. Phys. A **22**, 511 (1989).
- <sup>16</sup> P. B. Wiegmann, J. Phys. C **11**, 1583 (1978).
- <sup>17</sup> R. Rajaraman, *Solitons and Instantons* (North-Holland, Amsterdam, 1982).

## Figure Captions

1. The bands as a function of the energy  $E$  and the wave number  $q$  (near dimerization), both in units of  $\delta$ , taking  $\delta = 0.05$ . The numbers 1, 3 and 5 labeling the three biggest gaps are explained in the text.
2. A finer view of the bands as a function of  $E/\delta$  and  $q/\delta$ , for  $\delta = 0.05$ . A comparison with the second-order perturbation results is indicated by the six solid lines.
3. Semi-log plot of the widths  $\Delta E_n/\delta$  of the lowest four bands  $n = 0, 1, 2, 3$ . The points indicate the values obtained numerically for  $\delta = 0.05$ , while the solid lines (labeled by  $n$ ) show the WKB expressions in Eq. (21).
4. The density of states  $\rho$  as a function of  $E/\delta$  near dimerization. The solid and dashed lines show the behavior for  $q \rightarrow 0$  and  $q = 0$  respectively.
5. The bands as a function of  $(E - E_F)/\delta$  and  $q/\delta$ , for  $Q_0 = 2\pi/3$  and  $\delta = 0.4$ , with resolution  $dE = 10^{-5}$ .
6. Details of the bands as a function of  $(E - E_F)/\delta$  and  $q/\delta$ , near the top of the  $Q_0 = 2\pi/3$  gap for  $\delta = 0.4$ , with resolution  $dE = 10^{-8}$ .
7. The bands as a function of  $E$  and  $Q/(2\pi)$  for  $\delta = 0.4$ , with resolution  $dE = 10^{-4}$ .

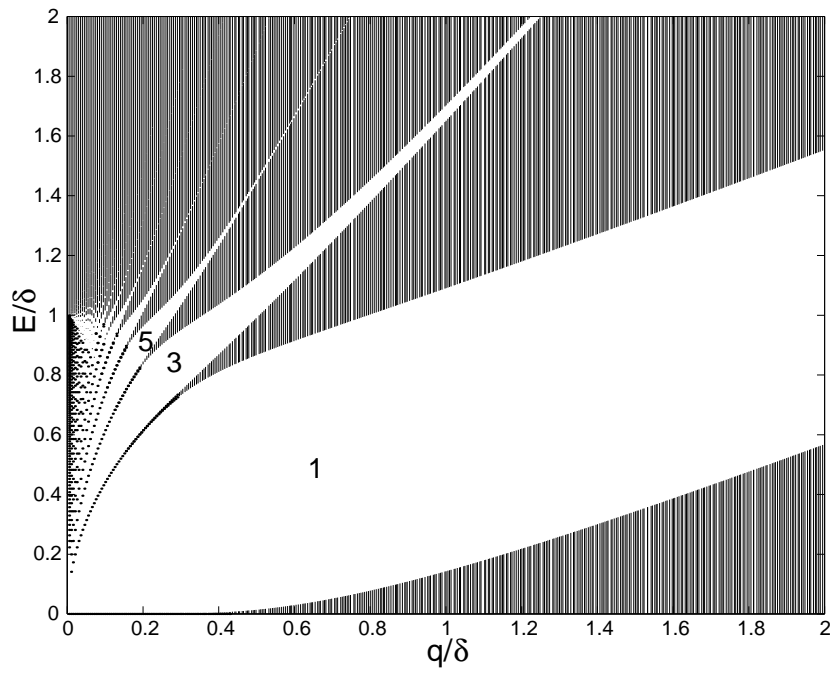


FIG. 1.

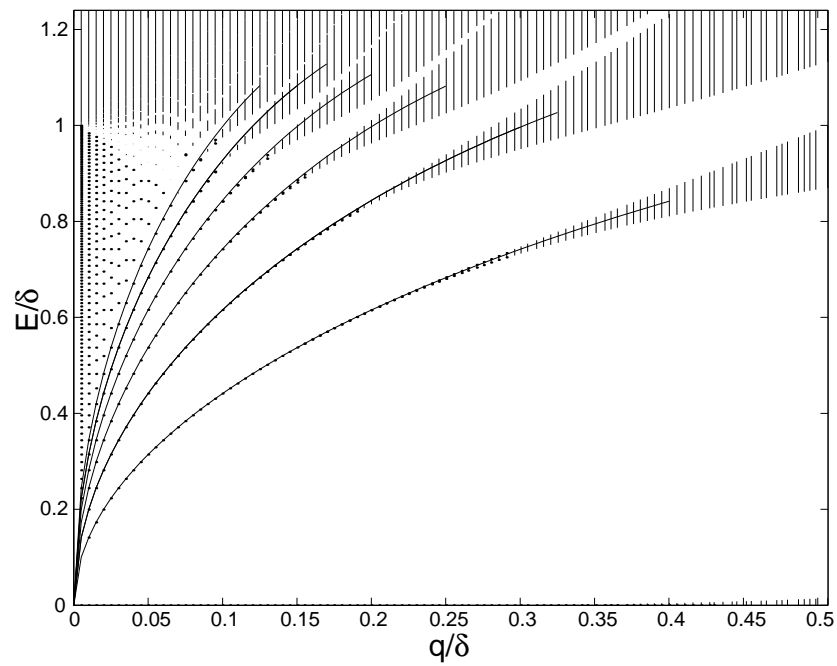


FIG. 2.

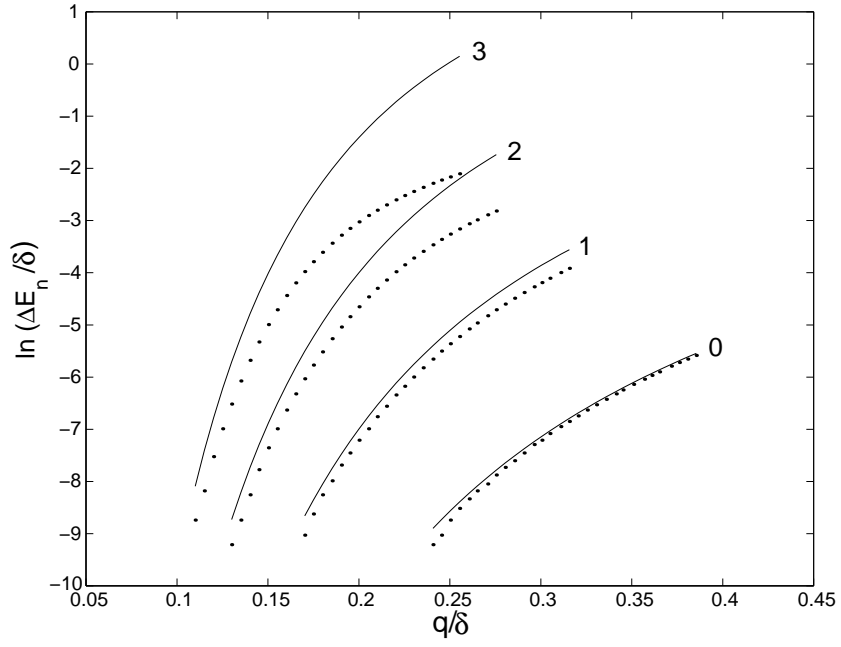


FIG. 3.

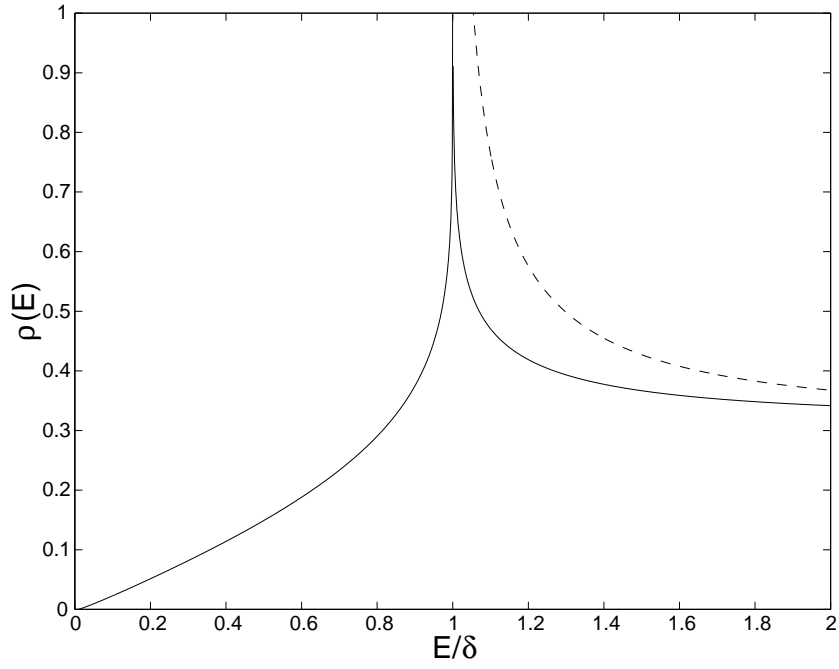


FIG. 4.

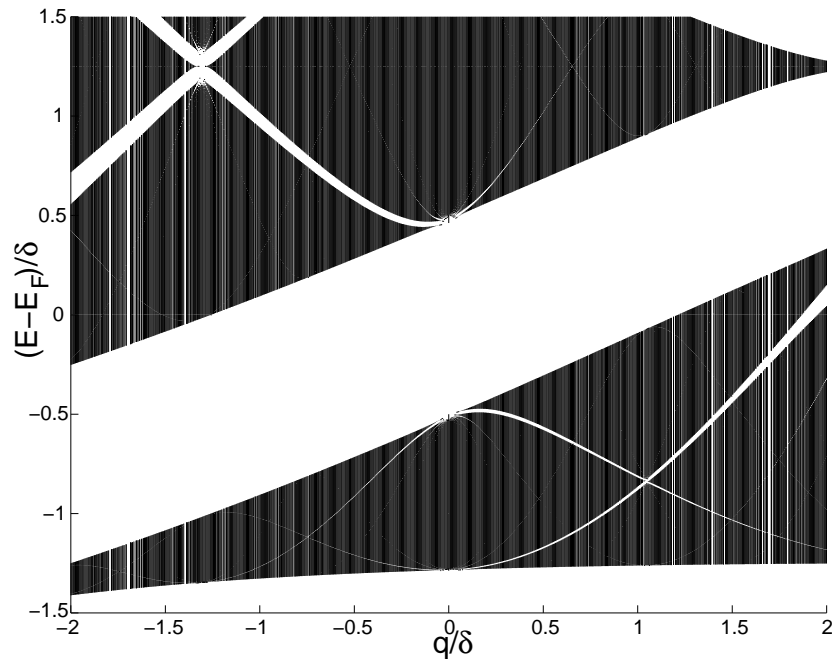


FIG. 5.

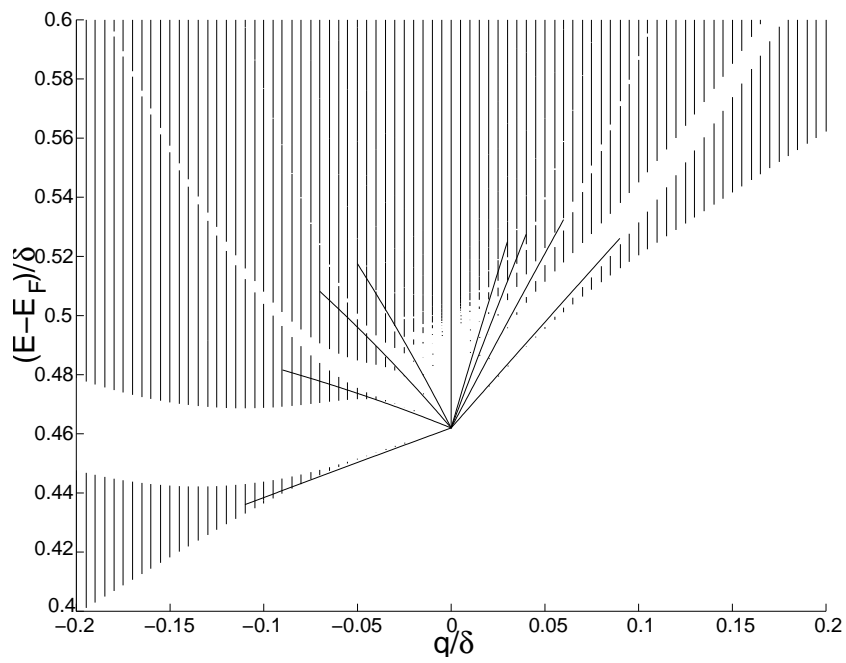


FIG. 6.

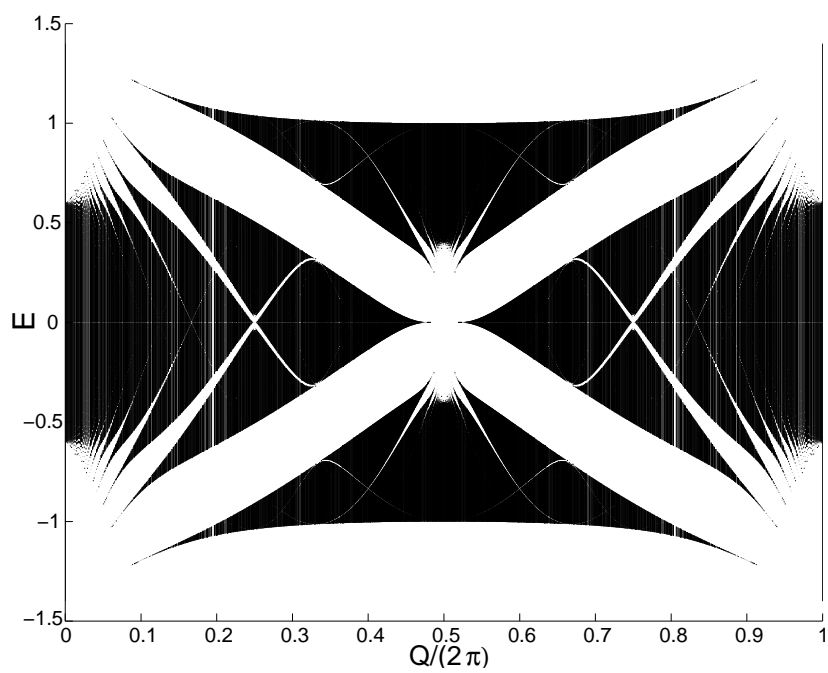


FIG. 7.